

Toward electrodynamics of unconventional phases of dilute nuclear matter

Armen Sedrakian

Frankfurt Institute for Advanced Studies, D-60438 Frankfurt am Main, Germany

E-mail: sedrakian@fias.uni-frankfurt.de

John W. Clark

Department of Physics and McDonnell Center for the Space Sciences, Washington University, St. Louis, Missouri 63130, USA

Centro de Investigação em Matemática e Aplicações, University of Madeira, 9020-105 Funchal, Madeira, Portugal

E-mail: jwc@wuphys.wustl.edu

Abstract. The phase diagram of isospin-asymmetrical nuclear matter may feature a number of unconventional phases, which include the translationally and rotationally symmetric, but isospin-asymmetrical BCS condensate, the current-carrying Larkin-Ovchinnikov-Fulde-Ferrell (LOFF) phase, and the heterogeneous phase-separated phase. Because the Cooper pairs of the condensate carry a single unit of charge, these phases are charged superconductors and respond to electromagnetic gauge fields by either forming domains (type-I superconductivity) or quantum vortices (type-II superconductivity). We evaluate the Ginzburg-Landau (GL) parameter across the phase diagram and find that the unconventional phases of isospin-asymmetrical nuclear matter are good type-II superconductors and should form Abrikosov vortices with twice the quantum of magnetic flux. We also find that the LOFF phase at the boundary of the transition to the type-I state, with the GL parameter being close to the critical value $1/\sqrt{2}$.

1. Introduction

Understanding superconducting phases of nuclear matter at sub-saturation densities is a challenging many-body physics problem. The attraction in the nuclear force is responsible for the formation of nuclear clusters, as well as condensates of Bardeen-Cooper-Schrieffer (BCS) type at low temperatures, with significant implications for the physics of supernovae and neutron stars. It has been conjectured such systems can exhibit the celebrated BCS-BEC transition [1], i.e., a transformation of loosely-bound Cooper pairs at weak coupling to bound dimers at strong coupling that form a Bose-Einstein condensate (BEC) [2, 3, 4, 5, 6, 7, 8, 9, 10]. However, these nuclear systems are isospin asymmetric, which means that the isoscalar neutron-proton (np) pairing is disrupted by the mismatch in the Fermi surfaces of protons and neutrons [11].

In a recent series of papers [12, 13, 14], the combined effects of the BCS-BEC crossover and mismatched Fermi surfaces have been studied in the phase diagram of nuclear and neutron matter, see also the reviews [15, 16]. The coupled equations for the gap and the densities of the constituents (neutrons and protons) have been solved allowing for (i) the ordinary BCS state,

(ii) its low-density asymptotic counterpart BEC state, and (iii) two phases that emerge once there is finite isospin asymmetry, namely the current-carrying phase (LOFF phase) and the spatially separated (PS-BCS) phase. The strong-coupling regime features the phase-separated BEC (PS-BEC) phase. Another important characteristic of these phases – the coherence length ξ – was extracted microscopically from the wave functions of the Cooper pairs, thus avoiding the standard definition which is valid only in the BCS limit.

The present contribution focuses on the electromagnetic response of the phases indicated above, which arises from the fact that the proton in an np Cooper pair carries a unit of charge. For this purpose we evaluate the penetration depth λ of the magnetic field in various regions of the phase diagram and deduce the Ginzburg-Landau (GL) parameter $\kappa = \lambda/\xi$. We then use the GL criterion to establish the type of the superconductivity realized in the phase diagram.

We note here that the type-II versus type-I superconductivity of the S -wave proton condensate in the core of a neutron star has been widely discussed in the literature, see for the recent work [17, 18, 19, 20, 21, 22] and for a recent review Ref. [23]. The proton superfluid contributes at most 10-15 percent to the density of the core, therefore its actual density is of the same order as that of the neutron-proton condensate considered here. The main differences arise through larger gaps in the present case, which lead to smaller coherence lengths, and the charges that the condensate carry (a unit of charge in the present case).

This contribution is structured as follows. In Sec. 2 we give a brief review of the theory of asymmetrical nuclear matter and discuss the resulting phase diagram. In Sec. 3 we address the electrodynamics of the superconducting state; we evaluate the GL parameter using input from our previous microscopic studies along with a new computation of the penetration depth. In Section 4 we collect our conclusions and consider related perspectives.

2. Review of the phase diagram

Superfluid nuclear matter can be described in terms of the Nambu-Gor'kov propagators, which from a matrix

$$i \begin{pmatrix} G_{12}^+ & F_{12}^- \\ F_{12}^+ & G_{12}^- \end{pmatrix} = \begin{pmatrix} \langle T_\tau \psi_1 \psi_2^+ \rangle & \langle T_\tau \psi_1 \psi_2 \rangle \\ \langle T_\tau \psi_1^+ \psi_2^+ \rangle & \langle T_\tau \psi_1^+ \psi_2 \rangle \end{pmatrix}, \quad (1)$$

where $x = (t, \mathbf{r})$ denotes the continuous temporal-spatial variable and Greek indices label discrete spin and isospin variables. Each operator in Eq. (1) can be viewed as a bi-spinor, i.e., $\psi_\alpha = (\psi_{n\uparrow}, \psi_{n\downarrow}, \psi_{p\uparrow}, \psi_{p\downarrow})^T$, where the symbols \uparrow, \downarrow label a particle's spin and the indices n, p label its isospin.

In energy-momentum space the elements of the matrix (1) are given by

$$G_{n/p}^\pm = \frac{ik_\nu \pm \epsilon_{p/n}^\mp}{(ik_\nu - E_{\mp/\pm}^+)(ik_\nu + E_{\pm/\mp}^-)}, \quad (2)$$

$$F_{np}^\pm = \frac{-i\Delta}{(ik_\nu - E_\pm^+)(ik_\nu + E_\mp^-)}, \quad (3)$$

$$F_{pn}^\pm = \frac{i\Delta}{(ik_\nu - E_\mp^+)(ik_\nu + E_\pm^-)}, \quad (4)$$

where the four branches of the quasiparticle spectrum are given by

$$E_r^a = \sqrt{E_S^2 + \Delta^2} + r\delta\mu + aE_A, \quad (5)$$

in which $a, r \in \{+, -\}$. Here

$$E_S = \frac{Q^2/4 + k^2}{2m^*} - \bar{\mu}, \quad E_A = \frac{\mathbf{k} \cdot \mathbf{Q}}{2m^*}, \quad (6)$$

are the symmetrical and anti-symmetrical parts of the quasiparticle spectrum, $\bar{\mu} \equiv (\mu_n + \mu_p)/2$, m^* is the effective mass of nucleon, and \mathbf{Q} is the center-of-mass momentum of the Cooper pairs.

The anomalous self-energy (pairing-gap) evaluated in the standard fashion to lowest order in the neutron-proton interaction $V(\mathbf{k}, \mathbf{k}')$ is expressed as

$$\begin{aligned} \Delta(\mathbf{k}, \mathbf{Q}) &= \frac{1}{4\beta} \int \frac{d^3 k'}{(2\pi)^3} \sum_{\nu} V(\mathbf{k}, \mathbf{k}') \\ &\quad \text{Im} \left[F_{np}^+(k'_{\nu}, \mathbf{k}', \mathbf{Q}) + F_{np}^-(k'_{\nu}, \mathbf{k}', \mathbf{Q}) - F_{pn}^+(k'_{\nu}, \mathbf{k}', \mathbf{Q}) - F_{pn}^-(k'_{\nu}, \mathbf{k}', \mathbf{Q}) \right], \end{aligned} \quad (7)$$

which yields, after partial-wave expansion and computation of the Matsubara sums,

$$\Delta_l(Q) = \frac{1}{4} \sum_{a,r,l'} \int \frac{d^3 k'}{(2\pi)^3} V_{l,l'}(k, k') \frac{\Delta_{l'}(k', Q)}{2\sqrt{E_S^2(k') + \Delta^2(k', Q)}} [1 - 2f(E_a^r)], \quad (8)$$

where $V_{l,l'}(k, k')$ is now the interaction in the 3S_1 - 3D_1 partial wave, $f(\omega) = 1/[\exp(\omega/T) + 1]$, and $\Delta^2 = \sum_l \Delta_l^2$.

The densities of neutrons and protons are obtained from the propagator after phase-space integration and summation over the discrete (spin-isospin) variables:

$$\begin{aligned} \rho_{n/p}(\mathbf{Q}) &= \frac{2}{\beta} \int \frac{d^3 k}{(2\pi)^3} \sum_{\nu} G_{n/p}^+(k_{\nu}, \mathbf{k}, \mathbf{Q}) \\ &= 2 \int \frac{d^3 k}{(2\pi)^3} \left[\frac{1}{2} \left(1 + \frac{E_S}{\sqrt{E_S^2 + \Delta^2}} \right) f(E_{\mp}^+) + \frac{1}{2} \left(1 - \frac{E_S}{\sqrt{E_S^2 + \Delta^2}} \right) f(-E_{\pm}^-) \right]. \end{aligned} \quad (9)$$

In writing the thermodynamic quantities we distinguish the spatially homogeneous and inhomogeneous cases and label the superfluid (S) or unpaired (N) quantities correspondingly. The free energies of the homogeneous phases can then be simply written as

$$F_S = E_S - TS_S, \quad F_N = E_N - TS_N, \quad (10)$$

where E is the internal energy (statistical average of the system Hamiltonian) and S denotes the entropy. The free energy of the heterogeneous superfluid phase (i.e. the phase in which there is a separation of the normal and superfluid phases) is given by

$$\mathcal{F}(x, \alpha) = (1 - x)F_S(\alpha = 0) + xF_N(\alpha \neq 0), \quad (Q = 0), \quad (11)$$

where x here denotes the filling fraction of the unpaired component and

$$\alpha = \frac{\rho_n - \rho_p}{\rho_n + \rho_p} \quad (12)$$

is the density asymmetry. The net density is given by $\rho = \rho_n + \rho_p$.

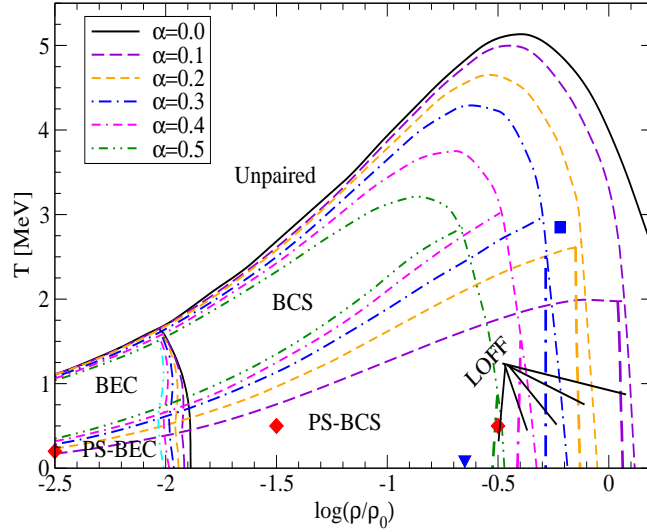


Figure 1. Phase diagram of dilute nuclear matter in the temperature-density plane for several isospin asymmetries α according to Refs. [12, 13]. The density is normalized to the nuclear saturation density. The phase diagram includes the unpaired phase, the BCS (BEC) phase, the LOFF phase, and the PS-BCS (PS-BEC) phase. For each asymmetry there are two tri-critical points, one of which is always a Lifshitz point [12, 13]. There is a single tetra-critical point in the phase diagram shown by the square dot. Note that the LOFF phase exists in the lower right corner of the phase diagram. The boundaries between BCS and BEC phases are identified by the change of sign of the average chemical potential $\bar{\mu}$. The diamonds mark the values of the density and temperature appearing in Table 1, these being chosen as representative of the three coupling regimes.

There are four possible states that can appear in the temperature-density phase diagram:

$$\begin{aligned}
 Q = 0, \quad \Delta \neq 0, \quad x = 0, \quad & \text{BCS phase,} \\
 Q \neq 0, \quad \Delta \neq 0, \quad x = 0, \quad & \text{LOFF phase,} \\
 Q = 0, \quad \Delta \neq 0, \quad x \neq 0, \quad & \text{PS phase,} \\
 Q = 0, \quad \Delta = 0, \quad x = 1, \quad & \text{unpaired phase.}
 \end{aligned} \tag{13}$$

Clearly, the phase with lowest free energy at any given temperature and density corresponds to the ground state of the nuclear matter. Their locations in the phase diagram are shown in Fig. 1 for several values of isospin asymmetry α . One can identify four different phases classified according to Eq. (13): (a) The unpaired phase occupies the high-temperature region $T > T_{c0}$ of the phase diagram, where $T_{c0}(\rho)$ is the critical temperature of the normal/superfluid phase transition at $\alpha = 0$. (b) The current-carrying LOFF phase is located in the lower right corner, corresponding to low temperatures and high densities. (c) The PS phase occupies the lower left corner, which corresponds to low densities and low temperatures. As the temperature is increased, these last two phases transform into (d) the isospin-asymmetrical BCS phase.

To quantify the BCS-BEC crossover, we define three regimes of coupling which we express in terms of densities. The strong-coupling regime (SCR) corresponds to the low-density limit where well-defined deuterons exist. The weak-coupling regime (WCR) corresponds to the high-density limit where well-defined Cooper pairs are formed. The regime intermediate between these domains is called the intermediate-coupling regime (ICR). Representative points in these regimes are indicated by diamonds in Fig. 1.

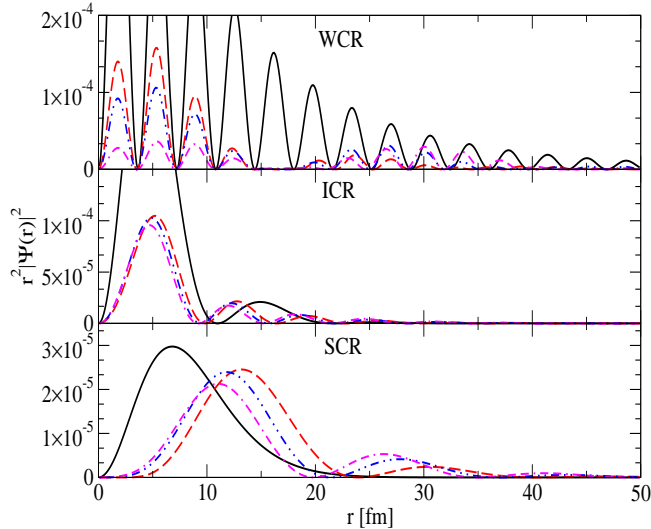


Figure 2. Dependence of $r^2|\Psi(r)|^2$ on r for the three coupling regimes [13]. (See Table 1 for corresponding values of density and temperature). For the asymmetry parameter we consider values $\alpha = 0$ (black, solid), 0.1 (red, long-dashed), 0.2 (blue, dash–double-dotted) and 0.3 (violet, double-dash-dotted).

3. Evaluating the Ginzburg-Landau parameter

BCS superconductors are characterized by at least three distinct length scales: (i) the *London penetration depth* λ , (ii) the *coherence length* ξ , and (iii) the mean interparticle distance d . The ratio of two of these scales defines the Ginzburg-Landau (GL) parameter: $\kappa = \lambda/\xi$. In the range $1/\sqrt{2} < \kappa < \infty$, the material is a type-II superconductor; otherwise it is type-I. In conventional type-II superconductors with Cooper charge $2e$ the magnetic field is carried by electromagnetic vortices with quantum flux $\phi_0 = \pi\hbar c/e$.

We now review the evaluation the coherence length, which can be related to the root-mean-square radius of the Cooper-pair wave function, defined as [12, 13]

$$\langle r^2 \rangle = \int d^3r r^2 |\Psi(\mathbf{r})|^2, \quad (14)$$

where $\Psi(\mathbf{r})$ is the Cooper-pair wave function. Fig. 2 shows the integrand of Eq. (14), i.e., the quantity $r^2|\Psi(\mathbf{r})|^2$. The spatial correlation in the SCR is found to display a single peak for $\alpha = 0$, which clearly indicates a tightly bound state at the origin. The residual oscillations (for finite asymmetries) indicate that there is no single bound state. The increasingly oscillatory behavior of the function $r^2|\Psi(\mathbf{r})|^2$ in the ICR is consistent with the notion of a transition from the BEC to the BCS regime. In the WCR, strong oscillations are observed, reflecting the coherence of the BCS state over large distances.

The coherence length, i.e., the spatial extension of a Cooper pair, is then defined as

$$\xi_{\text{rms}} = \sqrt{\langle r^2 \rangle}. \quad (15)$$

In the weak-coupling BCS regime the coherence length is given by the well-known analytical formula

$$\xi_a = \frac{\hbar^2 k_F}{\pi m^* \Delta}. \quad (16)$$

	$\log_{10}(\rho/\rho_0)$	k_F [fm $^{-1}$]	T [MeV]	d [fm]	ξ_{rms} [fm]	ξ_a [fm]	λ [fm]	κ_{rms}	$\kappa_{\text{rms}}^{\text{LOFF}}$
WCR	-0.5	0.91	0.5	1.68	3.17	1.41	18.5	5.8	0.8
ICR	-1.5	0.42	0.5	3.61	0.94	1.25	30.5	32.4	-
SCR	-2.5	0.20	0.2	7.79	0.57	1.79	50.5	88.2	-

Table 1. For each of the three regimes of coupling strength, corresponding values are presented for the density ρ (in units of nuclear saturation density $\rho_0 = 0.16 \text{ fm}^{-3}$), Fermi momentum k_F , temperature T , mean interparticle distance d , and coherence parameters ξ_{rms} and ξ_a . At $\alpha = 0$ the values of the pairing gap Δ in the three regimes WCR, ICR, and SCR are respectively 9.39, 4.50, and 1.44 MeV, while the corresponding values of the effective mass (in units of the bare mass) are 0.903, 0.989, and 0.999. In the regime WCR, the LOFF phase is found in the vicinity of asymmetry $\alpha = 0.49$, at which $\Delta = 1.27 \text{ MeV}$ and $Q = 0.4 \text{ fm}^{-3}$.

Table 1 lists the values of coherence length in the three coupling regimes, as obtained from Eq. (15) and through the BCS formula (16). The corresponding values of the mean interparticle distance listed in the Table are determined from the density.

We now apply the macroscopic equations of electrodynamics of superconductors. Since neutron-proton Cooper pairs carry a single unit of charge rather than two, the relations between various quantities differ accordingly from those for ordinary superconductors. To keep track of these differences we denote the charge and mass of a Cooper pair by e_X and m_X .

The gauge invariant momentum associated with the Cooper wave function is given by

$$\mathbf{p} = m_X \mathbf{v} = \hbar \nabla \chi - \frac{e_X}{c} \mathbf{A}, \quad (17)$$

where χ the phase of the wave function and \mathbf{A} the vector potential. Taking the curl of equations (17) yields

$$\text{curl } \mathbf{p} = m_X \text{curl } \mathbf{v} = 2\pi \hbar n_\phi \boldsymbol{\nu} - \frac{e_X}{c} \mathbf{B}, \quad (18)$$

where n_ϕ stands for the number density of vortices, $\boldsymbol{\nu} = (\text{curl } \mathbf{v}) / |\text{curl } \mathbf{v}|$ and $\mathbf{B} = \text{curl } \mathbf{A}$. The Maxwell equation for the magnetic field is

$$\text{curl } \mathbf{B} = \frac{4\pi}{c} e n_c \mathbf{v}, \quad (19)$$

where n_c is number density of charge carriers. Taking the curl of Eq. (19), we find the analogue of the London equation

$$\text{curl curl } \mathbf{B} = \lambda^{-2} (\phi^* n_\phi \boldsymbol{\nu} - \mathbf{B}), \quad (20)$$

where

$$\lambda = \left[\frac{4\pi e e_X}{m_X c^2} n_c \right]^{1/2}, \quad \phi^* = \frac{2\pi \hbar c}{e_X}. \quad (21)$$

In the case of interest, we have $e_X = e$ and $m_X = 2m^*$, where m^* is a nucleon effective mass. Therefore,

$$\lambda = \left[\frac{\pi e^2}{m^* c^2} (1 - \alpha) \right]^{1/2}, \quad \phi^* = \frac{2\pi \hbar c}{e} = 2\phi_0, \quad (22)$$

where $n_c \equiv \rho_p = (1 - \alpha)\rho/2$ is the density of charge carriers. It is seen from (22) that the quantum vortices present in the neutron-proton condensate carry twice the quantum of magnetic flux.

The values of λ and corresponding values of κ are given in Table 1 for representative points in the the coupling regimes WCR, ICR, and SCR. The gap value $\Delta = 1.27$ MeV found for the LOFF phase is much smaller than its corresponding value in the BCS state. Accordingly, to obtain a value for the coherence length in the LOFF phase, we have rescaled the ξ_{rms} value appearing in the table for the WCR case by the ratio of the pairing gap in the BCS state to that in the LOFF state, which is $9.39/1.27$. This yields $\xi_{\text{rms}}^{\text{LOFF}} \simeq 23.4$ fm, which implies $\kappa_{\text{rms}}^{\text{LOFF}} = 0.8$. Since the GL parameter is very close to the critical value $1/\sqrt{2}$ this particular phase is close to the transition to a type-I superconducting state for values of the gap $\Delta \leq 1$ MeV.

4. Conclusions and perspectives

Low-density nuclear and neutron matter feature a rich phase diagrams in the presence of isospin asymmetry or spin polarization respectively. These phase diagrams may contain a number of phases: the translationally and rotationally symmetric, but spin/isospin polarized BCS phase, the BEC phase containing quasi-deuterons, the current-carrying LOFF phase, and the phase-separated phase.

In this contribution we have concentrated on the electrodynamics of these phases across the phase diagram derived in Refs. [12, 13]. We have evaluated the penetration depth of the magnetic field of nucleonic matter in various regions of the phase diagram and combined it with the microscopically computed coherence length to obtain the Ginzburg-Landau parameter. We find that in the entire region of the phase diagram considered here (with few exceptions, see below), the condensed phases are type-II superconductors which must form Abrikosov quantum vortices. However, because the neutron-proton Cooper pairs carry only a unit of charge, these vortices will carry twice the quantum of circulation ϕ_0 . This is the main feature distinguishing the neutron-proton condensate from ordinary “condensed matter” superconductors and the proton superfluid in the core of a neutron star. In addition, we find that the LOFF phase is at the point of transition between the type-I and type-II superconducting states for gap values of the order of MeV. Because sufficiently large asymmetries will suppress the gap to values $\Delta \leq 1$ MeV, it is clear that this phase may eventually turn into a type-I superconductor. This argument applies to practically any phase with asymmetry, as $\xi \rightarrow \infty$ when $\Delta(\alpha) \rightarrow 0$ and therefore one finds $\kappa \rightarrow 0$. However, the relevant values of Δ might be extremely small for other phases.

In this contribution we have followed an approach based on phenomenological Ginzburg-Landau theory. It would be interesting and informative to extend our study of the electrodynamics of neutron-proton condensates to the microscopic level by evaluating the response functions of the condensates to electromagnetic fields (photon) in terms of the Green’s functions introduced in Sec. 2.

Acknowledgments

We are grateful to Martin Stein and Xu-Guang Huang for collaboration on the topics covered in Sec. 2. AS is supported by the Deutsche Forschungsgemeinschaft (Grant No. SE 1836/4-1). JWC acknowledges research support from the McDonnell Center for the Space Sciences and expresses his thanks to Professor José Luís da Silva and his colleagues in the Centro de Investigação em Matemática e Aplicações during extended residence at the University of Madeira.

References

- [1] Nozières P and Schmitt-Rink S 1985 *J. Low Temp. Phys.* **59** 195–211
- [2] Alm T, Friman B L, Röpke G and Schulz H 1993 *Nuclear Phys. A* **551** 45–53
- [3] Baldo M, Lombardo U and Schuck P 1995 *Phys. Rev. C* **52** 975–985

- [4] Lombardo U, Nozières P, Schuck P, Schulze H J and Sedrakian A 2001 *Phys. Rev. C* **64** 064314
- [5] Sedrakian A and Clark J W 2006 *Phys. Rev. C* **73** 035803
- [6] Mao S, Huang X and Zhuang P 2009 *Phys. Rev. C* **79** 034304
- [7] Huang X G 2010 *Phys. Rev. C* **81** 034007
- [8] Isaule F, Arellano H F and Rios A 2016 *Phys. Rev. C* **94** 034004
- [9] Rubtsova O A, Kukulin V I, Pomerantsev V N and Müther H 2017 *Phys. Rev. C* **96** 034327
- [10] Fan H H, Krotscheck E and Clark J W 2017 *J. Low. Temp. Phys.* **189** 470–494
- [11] Sedrakian A and Lombardo U 2000 *Phys. Rev. Lett.* **84** 602–605
- [12] Stein M, Huang X G, Sedrakian A and Clark J W 2012 *Phys. Rev. C* **86** 062801
- [13] Stein M, Sedrakian A, Huang X G and Clark J W 2014 *Phys. Rev. C* **90** 065804
- [14] Stein M, Sedrakian A, Huang X G and Clark J W 2016 *Phys. Rev. C* **93** 015802
- [15] Stein M, Sedrakian A, Huang X G, Clark J W and Röpke G 2014 *J. Phys. Conf. Series* **496** 012008
- [16] Clark J W, Sedrakian A, Stein M, Huang X G, Khodel V A, Shaginyan V R and Zverev M V 2016 *J. Phys. Conf. Series* **702** 012012
- [17] Buckley K B, Metlitski M A and Zhitnitsky A R 2004 *Phys. Rev. Lett.* **92** 151102
- [18] Alford M, Good G and Reddy S 2005 *Phys. Rev. C* **72** 055801
- [19] Sedrakian A 2005 *Phys. Rev. D* **71** 083003
- [20] Alford M G and Good G 2008 *Phys. Rev. B* **78** 024510
- [21] Sinha M and Sedrakian A 2015 *Phys. Rev. C* **91** 035805
- [22] Haber A and Schmitt A 2017 *Phys. Rev. D* **95** 116016
- [23] Haskell B and Sedrakian A 2017 *ArXiv e-prints (Preprint 1709.10340)*